Editors' Suggestion

Charged Polaron Polaritons in an Organic Semiconductor Microcavity

Chiao-Yu Cheng,[1] Rijul Dhanker,[1] Christopher L. Gray,[2] Sukrit Mukhopadhyay,[3] Eric R. Kennehan,[2] John B. Asbury,[2] Anatoliy Sokolov,[3] and Noel C. Giebink[1,*]

[1]*Department of Electrical Engineering, The Pennsylvania State University, University Park, Pennsylvania 16802, USA*
[2]*Department of Chemistry, The Pennsylvania State University, University Park, Pennsylvania 16802, USA*
[3]*The Dow Chemical Company, 1776 Building, Midland, Michigan 48674, USA*

(Received 15 August 2017; revised manuscript received 27 September 2017; published 3 January 2018)

We report strong coupling between light and polaron optical excitations in a doped organic semiconductor microcavity at room temperature. Codepositing MoO_3 and the hole transport material 4, 4′-cyclohexylidenebis[*N*, *N*-bis(4-methylphenyl)benzenamine] introduces a large hole density with a narrow linewidth optical transition centered at 1.8 eV and an absorption coefficient exceeding 10^4 cm^{-1}. Coupling this transition to a Fabry-Pérot cavity mode yields upper and lower polaron polariton branches that are clearly resolved in angle-dependent reflectivity with a vacuum Rabi splitting $\hbar\Omega_R > 0.3$ eV. This result establishes a path to electrically control polaritons in organic semiconductors and may lead to increased polariton-polariton Coulombic interactions that lower the threshold for nonlinear phenomena such as polariton condensation and lasing.

DOI: 10.1103/PhysRevLett.120.017402

Exciton-photon polaritons that emerge in the strong light-matter coupling regime have been studied extensively using a variety of organic and inorganic semiconductors [1,2]. Strong excitonic transitions typically provide the matter resonance, whereas a variety of different optical modes (such as, e.g., Fabry-Pérot [1,2], photonic crystal defect [3], and surface plasmon modes [4]) can be used for the photonic resonance. Being comprised of charge neutral excitons and photons, the resulting polaritons are also spin-1 bosons that carry no charge, and therefore their motion cannot be manipulated directly with applied electric fields, except for relatively weak instances when polaritons carry a static dipole moment inherited from a spatially indirect exciton transition [5,6].

The possibility of strong coupling to a *charged* semiconductor excitation was initially demonstrated for trions (i.e., a complex consisting of an exciton bound to a free electron or hole) in CdTe and GaAs quantum wells [7,8]. Owing to their net charge, the resulting trion polaritons are expected to possess some unusual properties, such as a very large charge-to-mass ratio, the ability to control their motion with an electric field, and a vacuum Rabi splitting that depends on the square root of the electron density in the quantum well [9]. This species nonetheless remains challenging to study and even more difficult to exploit for practical applications, because their low binding energy (∼1 meV) demands operation at liquid He temperature and invariably leads to an admixture with the neutral exciton polariton [8,9].

Here, we demonstrate strong coupling between light and charge-carrying polaron optical excitations in an organic semiconductor at room temperature. We show that a radical cation transition of hole-doped 4, 4′-cyclohexylidenebis[*N*, *N*-bis(4-methylphenyl)benzenamine] (TAPC) can be strongly coupled to the optical field in a planar microcavity to yield polaron polariton states with a vacuum Rabi splitting >0.3 eV. This result should greatly expand the practical potential of charged polaritons and may also lead to increased Coulombic polariton-polariton interactions in organic semiconductors that reduce the threshold for nonlinear phenomena such as parametric amplification, Bose-Einstein condensation, and polariton lasing [10–16].

Strong coupling between light and free charge carriers is uniquely facilitated in organic semiconductors by intense, narrow linewidth cationic and anionic optical transitions inherited from their constituent molecules [17–21], in contrast to the broad and featureless free carrier absorption of inorganic semiconductors [22]. Figure 1 illustrates the notion of an organic polaron polariton and how it differs from a traditional exciton polariton. In the former case shown in Fig. 1(b), when an electron is removed from a molecule to form the radical cation, the neutral excitonic transition is typically replaced by two new polaronic transitions shown in blue [23–26]. In the solid state, the excitation of an electron from a lower-lying molecular orbital into the partially vacant highest occupied molecular orbital (HOMO) can equivalently be viewed as the excitation of a hole.

Figure 2(a) shows the molecular structure of TAPC alongside the optical transitions calculated for its cation via density functional theory (B3LYP/6-31g**) using a background dielectric constant of 2.5 [27,28]. The lowest energy transitions are all hole excitations, with one deep in the infrared (0.4 eV) originating from the HOMO-1 and several closely spaced in the visible (between 1.8 and 2.2 eV) associated with lower-lying molecular orbitals.

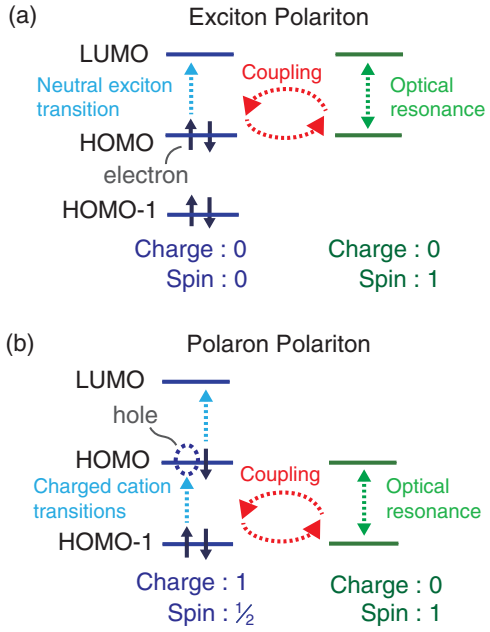

FIG. 1. Schematic showing the difference between a traditional organic semiconductor exciton polariton (a) and a polaron polariton (b). The former involves a Frenkel exciton transition between the highest occupied and lowest unoccupied molecular orbitals (HOMO and LUMO, respectively), whereas the latter involves a radical cation (or anion; not shown) transition, in this example, between the HOMO and a lower-lying molecular orbital.

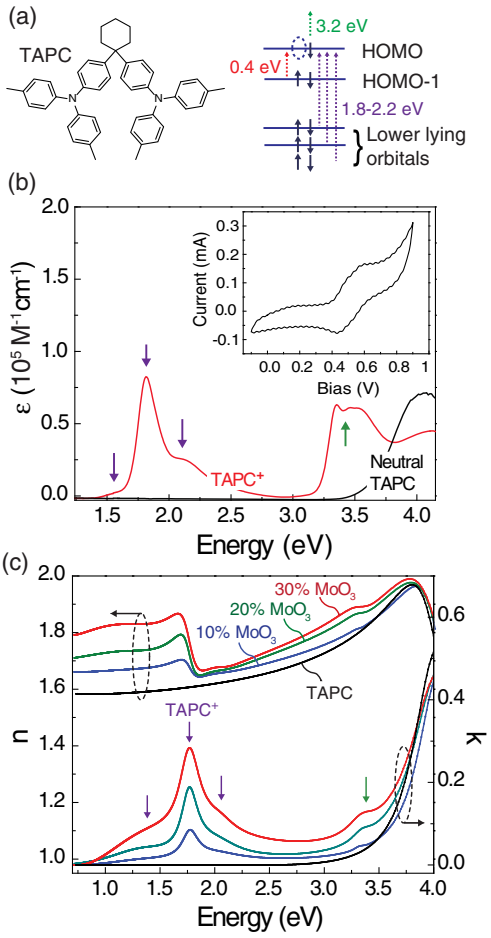

FIG. 2. (a) Molecular structure of TAPC together with the optical transitions calculated for its cation using the B3LYP functional. (b) Molar absorption coefficient of neutral TAPC (black line) and its cation ($TAPC^+$, red line). The solution consists of 50 μM TAPC dissolved in dichloromethane with a $0.5M$ tetrabutylammonium tetrafluoroborate ($TBABF_4$) electrolyte. The cation was created by electrochemically oxidizing TAPC for 40 min at 0.7 V with respect to a Ag/Ag^+ reference electrode in acetonitrile containing $0.01M$ $AgNO_3$ and $0.1M$ $TBABF_4$; the inset shows the associated cyclic voltammetry scan. (c) Complex refractive index optical constants $\tilde{n} = n + ik$, determined via variable angle spectroscopic ellipsometry for 40-nm-thick films of TAPC coevaporated with increasing concentrations of MoO_3 on a glass substrate. In (b) and (c), the $TAPC^+$ transitions in the 1.5–2.2 eV spectral range (purple arrows) are associated with excitation from low-lying orbitals into the partially occupied HOMO, whereas that at approximately 3.4 eV (green arrow) involves excitation from the HOMO into the LUMO as illustrated by the corresponding color arrows in (a).

Figure 2(b) shows that these transitions (indicated by purple arrows) are clearly observed in solution upon electrochemically oxidizing TAPC at its first oxidation potential shown in the inset. Based on these measurements, we estimate a peak molar extinction coefficient of $\varepsilon = 8.2 \times 10^4\ M^{-1}\,\mathrm{cm}^{-1}$ for the TAPC cation at 1.82 eV.

The same transitions are also observed in the solid state when TAPC is p-doped by coevaporating it with varying concentrations of MoO_3, as shown by the optical constant dispersions in Fig. 2(c). In this case, the large electron affinity of MoO_3 induces electron transfer from the TAPC HOMO, leaving behind a hole [29]. The polaron absorption band peaking at 1.77 eV is consistent with the cation absorption in solution [Fig. 2(b)] and is associated with hole excitations to states lying below the HOMO according to the computational model in Fig. 2(a). The slight redshift relative to the solution spectrum likely results from the solid-state solvation effect associated with the higher film refractive index (i.e., optical frequency dielectric constant).

The polaron extinction coefficient scales with the MoO_3 concentration up to approximately 30 wt %, where it peaks at $k = 0.28$ (corresponding to an absorption coefficient $\alpha = 4\pi k/\lambda = 5 \times 10^4\ \mathrm{cm}^{-1}$) before declining at higher concentrations. This trend is similar to that of the conductivity in other MoO_3-doped hole transport materials and is thought to result from Fermi level pinning within the disorder-induced HOMO density of states [29]. Based on an absorption cross section, $\sigma = 2.5 \times 10^{-16}\ \mathrm{cm}^2$ derived from the solution-phase molar absorption coefficient above, the $TAPC^+$ polaron density in the 30 wt % doped film is of the order of $10^{20}\ \mathrm{cm}^{-3}$.

To explore the strong coupling regime, we fabricated doped TAPC Fabry-Pérot microcavities with varying MoO_3 concentrations according to the structure: glass substrate/Ag(100 nm)/MoO_3 : TAPC(X nm)/Ag(17 nm), where X ranges from 175 nm for 10 wt % MoO_3 to 155 nm for 30 wt % MoO_3. Angle-dependent reflectivity measurements are carried out using collimated light (<1° divergence) from a laser-driven Xe light source filtered through a monochromator and detected synchronously with a photodiode and lock-in amplifier. Figures 3(a) and 3(b) show the s-polarized reflectivity spectra for cavities with 10 and 30 wt % MoO_3 concentration, respectively. In both cases, we observe two dips with a clear anticrossing evolution (shown by the red lines) about the bare polaron transition energy (vertical green dashed line) that correspond to upper and lower branch polariton modes. These data are in good agreement with transfer matrix modeling of the reflectivity (black dashed lines) based on the associated MoO_3:TAPC complex refractive index dispersions shown in Fig. 2(c).

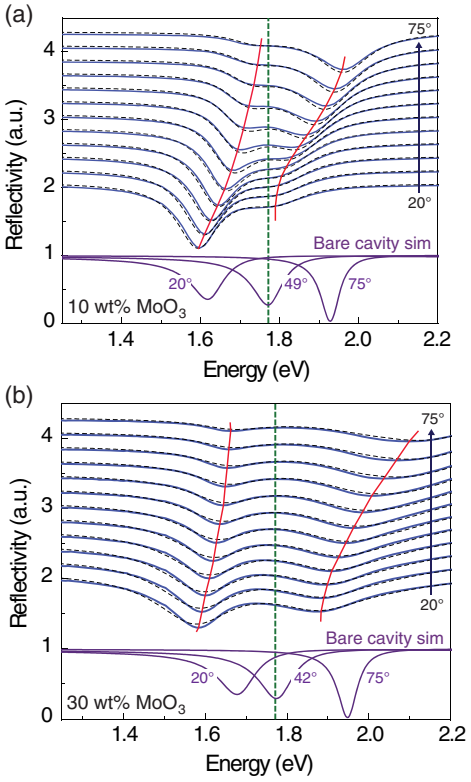

FIG. 3. Angle-dependent reflectivity spectra of microcavities containing (a) 10 wt % MoO_3:TAPC and (b) 30 wt % MoO_3:TAPC. The spectra (blue lines) are acquired at incidence angles ranging from 20° to 75° in 5° increments and are offset vertically from one another for clarity. The dashed black lines indicate the simulated reflectivity at each incidence angle based on the associated MoO_3:TAPC complex refractive index dispersions displayed in Fig. 2(c). The solid red lines are drawn as a guide to show the anticrossing behavior. The vertical dashed green line at 1.77 eV designates the bare polaron transition energy, and the purple reflectivity spectra at the bottom of each plot are the angle-dependent reflectivities simulated for the bare cavity.

The energy of each mode is extracted from the reflectivity data via Gaussian multipeak fitting, and the resulting dispersion is plotted for the 30 wt % MoO_3 sample in Fig. 4(a). There, the dispersion of the upper and lower polariton branches is well described by a 2×2 coupled oscillator Hamiltonian [1,2]:

$$\begin{bmatrix} E_\gamma & V \\ V & E_P \end{bmatrix} \begin{bmatrix} \alpha \\ \beta \end{bmatrix} = E \begin{bmatrix} \alpha \\ \beta \end{bmatrix}, \tag{1}$$

where $E_P = 1.77$ eV is the energy of the uncoupled polaron transition and $E_\gamma(\theta)$ is the energy of the bare photon mode computed at each incidence angle for an equivalent cavity with the background refractive index dispersion of MoO_3:TAPC estimated from ellipsometry in the absence of the cation transitions. The interaction energy V is determined by fitting the eigenvalues of Eq. (1) to the data in Fig. 4(a), which leads to a Rabi splitting $\hbar\Omega_R \approx 2V = 320 \pm 40$ meV, neglecting the cavity linewidth and homogeneous broadening of the polaron transition [30]. Figure 4(b) summarizes the Rabi splitting obtained without approximation for all of the different MoO_3 concentrations, demonstrating a linear variation with the square root of the polaron absorbance [i.e., $\Omega_R \propto (\alpha d)^{1/2}$, where d is the cavity thickness] as expected [1,2]. We note that, while the Rabi splitting of the 30 wt % MoO_3 cavity explicitly satisfies the nominal strong coupling condition $\Omega > \delta_P/2 + \delta_\gamma/2$, defined in terms of the bare cavity linewidth ($\delta_\gamma \sim 0.1$ eV full width at half maximum; see Fig. 3) and the polaron transition linewidth [$\delta_P \sim 0.38$ eV; see Fig. 2(c)] [4], the lower concentration cavities do not. The fact that the 10 wt % MoO_3 cavity strongly couples with a clearly resolved anticrossing in Fig. 3(a) despite not meeting this condition is due to the fact that polaritons tend to reflect the homogeneous, rather than inhomogeneous, linewidth of the underlying electronic transition [31,32]. In the present case, the polaron transition is dominated by inhomogeneous broadening; we estimate its homogeneous linewidth to be less than 5 meV based on an excited state lifetime of ~1 ps measured via ultrafast transient absorption.

Taken together, these data demonstrate that polaron polaritons are readily achievable at room temperature using organic semiconductors. This species is distinct from trion polaritons [8,9] as well as alternative multiparticle notions of a polaron polariton [33], and it carries a number of implications that are interesting to consider. First, the dependence of the Rabi splitting on the polaron density established in Fig. 4(b) should make it possible to electrically gate the strong coupling regime in much the same manner as intersubband systems [34], which are probably the closest inorganic semiconductor analog. Polaron densities exceeding 10^{18} cm^{-3} (i.e., comparable to that used

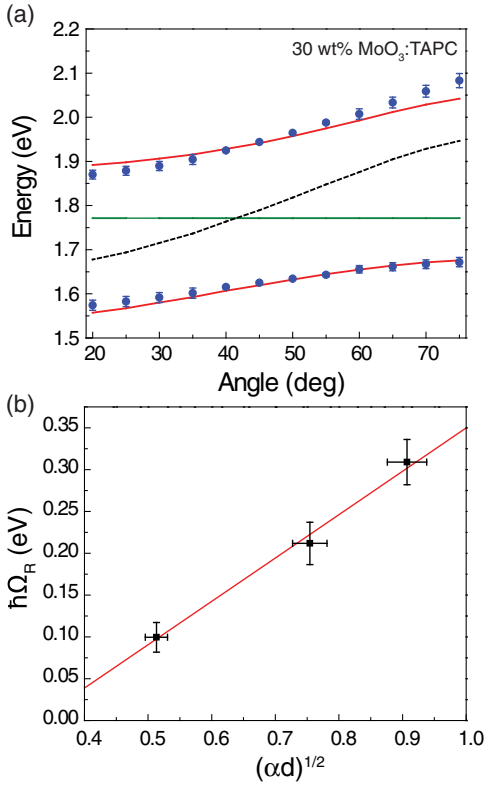

FIG. 4. (a) Polariton dispersion for the 30 wt % MoO_3:TAPC cavity extracted from the reflectivity data of Fig. 3(b). The green solid line indicates the uncoupled polaron transition energy, the black dashed line denotes the bare cavity mode dispersion, and the red solid lines are a fit from the coupled oscillator model described in the text. (b) Linear fit (red line) to the dependence of the Rabi splitting on the square root of the polaron absorbance determined for the 10, 20, and 30 wt % MoO_3:TAPC microcavities.

here) are readily achievable in organic thin film transistors [35], though the nanometer thickness of typical accumulation layers will require the photon mode to be tightly confined near the organic semiconductor–gate dielectric interface. Beyond electrostatic control over their energy, charged polaritons have been predicted to accelerate in an applied electric field [9], and they may offer interesting magnetic field effects owing to the unpaired half-integer spin of the underlying radical cations or anions [36].

It is also possible that polaron polaritons will interact with one another more strongly than exciton polaritons, which is significant because it would lower the threshold for nonlinear polariton phenomena such as parametric amplification, Bose-Einstein condensation, and lasing [13,15,16]. While no direct Coulomb interaction is expected between them (i.e., only the excitation of polarons propagates, so the position of polarons relative to one another, and thus their Coulomb repulsion, does not change as two polaritons approach one another), there may be secondary effects that are nonetheless significant. For example, the electronic polarization of the surrounding molecules may change in the transition between polaron ground and excited states, since the wave function of the latter is typically more extended. Owing to the low dielectric constant of organic materials, this would provide the basis for a long-range Coulombic polariton-polariton interaction, which is normally negligible for organic semiconductor exciton polaritons.

Finally, it is interesting to consider the extent to which strong polaron-photon coupling might alter organic semiconductor electrical properties, as reported previously for neutral exciton polariton systems [37,38]. Polaron polaritons, by comparison, arguably offer a more direct link to electrical properties, since the excitation of free charge carriers themselves is shared via the cavity mode. This may give rise to, for example, enhanced photoconductivity in a polaron polariton system that is closely analogous to enhanced exciton conductance that has been predicted for exciton polariton systems [39].

In summary, we have strongly coupled light in a Fabry-Pérot microcavity to a polaron optical transition of the organic semiconductor TAPC. By doping TAPC with MoO_3 to introduce a large density of holes, we achieve a hole absorption coefficient exceeding 10^4 cm^{-1} with a sufficiently narrow linewidth to resolve Rabi splittings in excess of 0.3 eV at room temperature. The resulting polaron polaritons are unique to organic semiconductors and may offer enhanced nonlinearities as well as a pathway to exploit charged polaritons in practical optoelectronic applications.

We thank S. Kéna-Cohen and J. Feist for helpful discussions. This work was supported in part by the Air Force Office of Scientific Research under Grant No. FA-9550-14-1-0301 and by the National Science Foundation under Grant No. DMR-1654077. E. R. K. and J. B. A. are grateful for support from The Dow Chemical Company under the University Project Initiative No. 225559AG.

*ncg2@psu.edu

[1] M. S. Skolnick, T. A. Fisher, and D. M. Whittaker, Strong coupling phenomena in quantum microcavity structures, Semicond. Sci. Technol. **13**, 645 (1998).
[2] R. J. Holmes and S. R. Forrest, Strong exciton-photon coupling in organic materials, Org. Electron. **8**, 77 (2007).
[3] H. M. Gibbs, G. Khitrova, and S. W. Koch, Exciton-polariton light-semiconductor coupling effects, Nat. Photonics **5**, 273 (2011).
[4] P. Torma and W. L. Barnes, Strong coupling between surface plasmon polaritons and emitters: A review, Rep. Prog. Phys. **78**, 013901 (2015).
[5] G. Christmann, A. Askitopoulos, G. Deligeorgis, Z. Hatzopoulos, S. I. Tsintzos, P. G. Savvidis, and J. J. Baumberg, Oriented polaritons in strongly-coupled asymmetric double quantum well microcavities, Appl. Phys. Lett. **98**, 081111 (2011).

[6] P. Cristofolini, G. Christmann, S. I. Tsintzos, G. Deligeorgis, G. Konstantinidis, Z. Hatzopoulos, P. G. Savvidis, and J. J. Baumberg, Coupling quantum tunneling with cavity photons, Science **336**, 704 (2012).
[7] T. Brunhes, R. André, A. Arnoult, J. Cibert, and A. Wasiela, Oscillator strength transfer from X to X+ in a CdTe quantum-well microcavity, Phys. Rev. B **60**, 11568 (1999).
[8] R. Rapaport, R. Harel, E. Cohen, A. Ron, E. Linder, and L. N. Pfeiffer, Negatively Charged Quantum Well Polaritons in a GaAs/AlAs Microcavity: An Analog of Atoms in a Cavity, Phys. Rev. Lett. **84**, 1607 (2000).
[9] R. Rapaport, E. Cohen, A. Ron, E. Linder, and L. N. Pfeiffer, Negatively charged polaritons in a semiconductor microcavity, Phys. Rev. B **63**, 235310 (2001).
[10] T. Byrnes, N. Y. Kim, and Y. Yamamoto, Exciton-polariton condensates, Nat. Phys. **10**, 803 (2014).
[11] M. D. Fraser, S. Hoefling, and Y. Yamamoto, Physics and applications of exciton-polariton lasers, Nat. Mater. **15**, 1049 (2016).
[12] M. Saba, C. Ciuti, J. Bloch, V. Thierry-Mieg, R. André, L. S. Dang, S. Kundermann, A. Mura, G. Bongiovanni, and J. L. Staehli, High-temperature ultrafast polariton parametric amplification in semiconductor microcavities, Nature (London) **414**, 731 (2001).
[13] D. Sanvitto and S. Kena-Cohen, The road towards polaritonic devices, Nat. Mater. **15**, 1061 (2016).
[14] J. Kasprzak, M. Richard, S. Kundermann, A. Baas, P. Jeambrun, J. M. J. Keeling, F. M. Marchetti, M. H. Szymanska, R. Andre, and J. L. Staehli, Bose-Einstein condensation of exciton polaritons, Nature (London) **443**, 409 (2006).
[15] K. S. Daskalakis, S. A. Maier, R. Murray, and S. Kéna-Cohen, Nonlinear interactions in an organic polariton condensate, Nat. Mater. **13**, 271 (2014).
[16] S. Kéna-Cohen and S. R. Forrest, Room-temperature polariton lasing in an organic single-crystal microcavity, Nat. Photonics **4**, 371 (2010).
[17] M. Pope and C. E. Swenberg, *Electronic Processes in Organic Crystals and Polymers*, 2nd ed. (Oxford University, New York, 1999).
[18] P. Balk, G. J. Hoijtink, and J. W. H. Schreurs, Electronic spectra of mono-and di-negative aromatic ions, Recl. Trav. Chim. **76**, 813 (1957).
[19] G. J. Hoijtink and P. J. Zandstra, Polarization of electronic transitions in aromatic hydorcarbon molecules and their mono-and di-valent ions, Mol. Phys. **3**, 371 (1960).
[20] T. Shida and S. Iwata, Electronic spectra of ion radicals and their molecular orbital interpretation. III. Aromatic hydrocarbons, J. Am. Chem. Soc. **95**, 3473 (1973).
[21] P. M. Beaujuge and J. R. Reynolds, Color control in π-conjugated organic polymers for use in electrochromic devices, Chem. Rev. **110**, 268 (2010).
[22] L. A. Coldren and S. W. Corzine, *Diode Lasers and Photonic Integrated Circuits* (Wiley, New York, 1995).
[23] A. Kohler and H. Bassler, *Electronic Processes in Organic Semiconductors* (Wiley-VCH, New York, 2015), p. 161.
[24] J. L. Bredas and G. B. Street, Polarons, bipolarons, and solitons in conducting polymers, Acc. Chem. Res. **18**, 309 (1985).
[25] J. Cornil and J.-L. Brédas, Nature of the optical transitions in charged oligothiophenes, Adv. Mater. **7**, 295 (1995).
[26] J. A. E. H. van Haare, E. E. Havinga, J. L. J. van Dongen, R. A. J. Janssen, J. Cornil, and J.-L. Brédas, Redox states of long oligothiophenes: Two polarons on a single chain, Chem. Eur. J. **4**, 1509 (1998).
[27] S. Zheng, S. Barlow, C. Risko, T. L. Kinnibrugh, V. N. Khrustalev, S. C. Jones, M. Y. Antipin, N. M. Tucker, T. V. Timofeeva, and V. Coropceanu, Isolation and crystal structures of two singlet bis (triarylamine) dications with nonquinoidal geometries, J. Am. Chem. Soc. **128**, 1812 (2006).
[28] S. Barlow, C. Risko, S. A. Odom, S. Zheng, V. Coropceanu, L. Beverina, J.-L. Brédas, and S. R. Marder, Tuning delocalization in the radical cations of 1, 4-bis [4-(diarylamino) styryl] benzenes, 2, 5-bis [4-(diarylamino) styryl] thiophenes, and 2, 5-bis [4-(diarylamino) styryl] pyrroles through substituent effects, J. Am. Chem. Soc. **134**, 10146 (2012).
[29] M. Kröger, S. Hamwi, J. Meyer, T. Riedl, W. Kowalsky, and A. Kahn, P-type doping of organic wide band gap materials by transition metal oxides: A case-study on molybdenum trioxide, Org. Electron. **10**, 932 (2009).
[30] L. Tropf, C. P. Dietrich, S. Herbst, A. L. Kanibolotsky, P. J. Skabara, F. Würthner, I. D. W. Samuel, M. C. Gather, and S. Höfling, Influence of optical material properties on strong coupling in organic semiconductor based microcavities, Appl. Phys. Lett. **110**, 153302 (2017).
[31] R. Houdré, R. P. Stanley, and M. Ilegems, Vacuum-field Rabi splitting in the presence of inhomogeneous broadening: Resolution of a homogeneous linewidth in an inhomogeneously broadened system, Phys. Rev. A **53**, 2711 (1996).
[32] A. V. Kavokin, Motional narrowing of inhomogeneously broadened excitons in a semiconductor microcavity: Semiclassical treatment, Phys. Rev. B **57**, 3757 (1998).
[33] M. Sidler, P. Back, O. Cotlet, A. Srivastava, T. Fink, M. Kroner, E. Demler, and A. Imamoglu, Fermi polaron-polaritons in charge-tunable atomically thin semiconductors, Nat. Phys. **13**, 255 (2017).
[34] A. A. Anappara, A. Tredicucci, F. Beltram, G. Biasiol, and L. Sorba, Controlling polariton coupling in intersubband microcavities, Superlattices Microstruct. **41**, 308 (2007).
[35] H. Klauk, Organic thin-film transistors, Chem. Soc. Rev. **39**, 2643 (2010).
[36] J. M. Lupton, D. R. McCamey, and C. Boehme, Coherent spin manipulation in molecular semiconductors: Getting a handle on organic spintronics, ChemPhysChem **11**, 3040 (2010).
[37] J. A. Hutchison, A. Liscio, T. Schwartz, A. Canaguier-Durand, C. Genet, V. Palermo, P. Samori, and T. W. Ebbesen, Tuning the work-function via strong coupling, Adv. Mater. **25**, 2481 (2013).
[38] E. Orgiu, J. George, J. A. Hutchison, E. Devaux, J. F. Dayen, B. Doudin, F. Stellacci, C. Genet, J. Schachenmayer, C. Genes, G. Pupillo, P. Samori, and T. W. Ebbesen, Conductivity in organic semiconductors hybridized with the vacuum field, Nat. Mater. **14**, 1123 (2015).
[39] J. Feist and F. J. Garcia-Vidal, Extraordinary Exciton Conductance Induced by Strong Coupling, Phys. Rev. Lett. **114**, 196402 (2015).